Chemistry of Metals and Alloys

Chem. Met. Alloys 16 (2023) 37-42
Ivan Franko National University of Lviv
http://publications.lnu.edu.ua/chemetal

Properties of thermally treated Ti/TiO_2 nanotubes: increased crystalline phase and carrier concentration

Olesia SHMYCHKOVA[1]*, Tatiana LUK'YANENKO[1], Alexander VELICHENKO[1]

[1] *Ukrainian State University of Chemical Technology, Gagarina Ave. 8, 49005 Dnipro, Ukraine*
* *Corresponding author. Tel.:* +380567462825*; e-mail: o_shmychkova@ukr.net*

Received October 13, 2023; accepted December 19, 2023
https://doi.org/10.30970/cma16.0432

As prepared Ti/TiO_2 materials exhibit a notable presence of X-ray amorphous compounds on the surface, likely corresponding to hydrated titanium oxides. The primary crystalline phase observed is titanium dioxide in the anatase form. Traces of metallic titanium are also found on the surface. There is an increase in the proportion of the crystalline phase, with a significant rise in the content of metallic titanium, accounting for approximately one-third of the composition upon thermal treatment at 500°C for 3 hours in an air atmosphere. Through partial electrochemical reduction of nanotubes, it is possible to obtain titanium suboxides with improved electrical conductivity. Subsequent cathodic reduction of nanotubes for one hour results in the uniform deposition of a galvanic coating composed of metallic platinum on the material's surface. The thermally treated Ti/TiO_2 nanotubes exhibit *n*-type semiconductor behavior, with a flat-band potential of -0.589 V and a carrier concentration of 6×10^{20} cm^{-3}. During thermal treatment, the flat-band potential and carrier concentration increase, possibly due to the more crystalline structure of the material. This structural change is accompanied by an increase in the proportion of metallic titanium, which acts as an electron donor. A similar phenomenon is observed when a discontinuous platinum coating is applied to the surface of reduced nanotubes. In this case, heat treatment causes platinum migration into the bulk of the composite, which, when dispersed within the oxide, further increases the number of carriers.

Carrier concentration / Thermal treatment / Phase composition / Nanotubes

1. Introduction

One of the most fascinating areas of modern science and technology is the study of nanomaterials and their potential applications in various industries [1]. One particularly captivating research direction is the synthesis and investigation of titanium dioxide nanotubes, which possess unique properties and offer a wide range of possibilities in different applications [1,2].

Titanium dioxide nanotubes are structures composed of layers of titanium and oxygen, forming a tubular shape. They have nanometer-scale dimensions, which make them particularly interesting for research and utilization in nanotechnology. One of the most common methods for synthesizing titanium oxide nanotubes is hydrothermal synthesis, which relies on a high-temperature and high-pressure environment [3]. Solvothermal, sol-gel, direct oxidation methods, chemical vapor deposition, electrodeposition, sonochemical and microwave methods have also been used to produce TiO_2 nanoparticles [4-7].

The ability of titanium dioxide nanotubes to absorb light and exhibit high surface activity makes them attractive for use in photocatalytic processes. However, their application as a photocatalyst is limited by their low quantum efficiency, weak separation of electron-hole pairs, and limited absorption spectrum in the ultraviolet region [8,9]. They can be employed for the decomposition of organic pollutants in water and air, as well as for solar photocatalysis. This opens up possibilities for developing efficient water and air purification systems, as well as utilizing renewable energy sources.

Titanium dioxide nanotubes also possess promising properties in the field of electronics and sensing. Their high electrical conductivity and unique structure enable their use in the creation of nanoelectronic devices, such as nanotransistors and nanosensors. These devices can have a broad range of applications, ranging from medical diagnostics and environmental monitoring to next-generation electronics [10].

In addition to this, titanium oxide nanotubes find applications in the field of catalysis, energy storage,

and conversion, where their unique properties contribute to enhanced efficiency and performance. However, most catalysts involved in cathodic processes have limited stability towards reverse current or at high anodic polarization, especially in the presence of chloride ions [11]. Current collectors made of carbon materials are rapidly destroyed, and metal and TiO_2 are passivated.

Overall, the synthesis of titanium dioxide nanotubes represents an exciting area of research with significant potential for various fields, including environmental remediation, electronics, and energy.

To address all the above-mentioned limitations, we propose a combined electrochemical-pyrolytic method of nanotube synthesis. This method can create a template with porous surface for subsequent electrodeposition of catalytic layers of platinum and palladium, which can be heat-treated in air atmosphere. The high number of cationic vacancies in the matrix and the deficiency of oxygen ions will significantly increase the mobility of platinum and palladium atoms during heat treatment, resulting in a composite with practically metal conductivity, high catalytic activity, selectivity, and extended service life.

2. Experimental

All the chemicals were analytical reagent grade. Composites were obtained by an original method, which includes stages of preliminary preparation of the titanium substrate [12,13]. Enhanced TiO_2 nanotubes were grown from the Ti substance followed by a double anodization and cathodization process [14-16] and galvanic platinization. Platinum was electrodeposited at 80°C at a cathodic current density of 10 mA cm^{-2} from 0.05 M K_2PtCl_6 + 1.5 M $NaNO_2$ + 100 g/L NH_3 [17]. The coating thickness was about 1 μm (~2 mg Pt per cm^2). Some samples were thermally treated under air in a tube furnace at 500°C for 1-3 h.

The surface morphology was studied by scanning electron microscopy (SEM) with a Tescan Vega 3 LMU device with an energy-dispersive X-ray microanalyzer Oxford Instruments Aztec ONE with an X-Max^{N}20 detector. X-Ray powder diffraction (XRPD) data were collected in the transmission mode on a STOE STADI P diffractometer with Cu $K\alpha_1$-radiation, a curved Ge(111) monochromator on the primary beam, $2\theta/\omega$-scan, angular range for data collection 20.000-110.225° 2θ with increment 0.015, linear position-sensitive detector with step of recording 0.480° 2θ and time per step 75-300 s, $U = 40$ kV, $I = 35$ mA, $T = 298$ K. A calibration procedure was performed utilizing SRM 640b (Si) and SRM 676 (Al_2O_3) NIST standards. Preliminary data processing and X-ray qualitative phase analysis were performed using the STOE WinXPOW and PowderCell program packages. The crystal structures of the phases were refined by the Rietveld method with the program FullProf.2k, applying a pseudo-Voigt profile function and isotropic approximation for the atomic displacement parameters, together with quantitative phase analysis.

The oxygen evolution reaction was investigated by steady-state polarization on a computer-controlled MTech PGP-550M potentiostat-galvanostat in different electrolytes, depending on the purpose of the experiment.

3. Results and discussion

Rutile is the most stable phase of TiO_2 at room temperature. It has a crystalline structure in which each titanium atom is surrounded by six oxygen atoms. Rutile has high density and hardness, as well as excellent optical properties, making it useful in solar cells and optical coatings. Anatase is another common phase of TiO_2. It has a more open crystalline structure than rutile. The titanium atoms are surrounded by five oxygen atoms, making anatase more reactive and having higher surface activity. Anatase is widely used in photocatalysis due to its high efficiency in decomposing organic pollutants under light exposure. Brookite is the third phase of TiO_2 but is less commonly found compared to rutile and anatase. It has a more complex crystalline structure and lower stability at high temperatures. Brookite also possesses good photocatalytic properties and finds applications in various fields, including solar cells and photocatalysts [18-20].

Each of these structures has its own characteristics and applications in different areas. The choice of a specific phase of TiO_2 depends on the particular application and desired material properties.

Furthermore, modifications can be made to these phases to enhance specific properties. Various synthesis and processing methods can alter the size, shape, and surface properties of TiO_2 particles, allowing for optimization in specific applications.

As depicted in Fig. 1, the morphology of the TiO_2 nanotubes showed nanotubes with an inner diameter in the range of 70-100 nm with a wall thickness of about 15-20 nm. One can see a nanocombed pattern of growth. The resulting nanotubes exhibit a uniform size distribution and high aspect ratios.

X-ray diffraction data revealed that the obtained nanotubes exhibit a significant amount of X-ray amorphous compounds on their surface, most likely hydrated titanium oxides. The primary crystalline phase present is titanium dioxide in the anatase form. There are trace amounts of metallic titanium on the surface. Thermal treatment of this material at 500°C for 3 h in an air atmosphere leads to an increase in the proportion of crystalline phase (Table 1).

In this case, the content of metallic titanium significantly increases, reaching approximately one-third of the composition. It should be noted that attempts to deposit metallic platinum on the surface of TiO_2 nanotubes *via* electrolysis were unsuccessful.

Even after thermal treatment, only localized coating deposition was observed in specific areas. Therefore, we performed a partial electrochemical reduction of the nanotubes to obtain more electrically conductive titanium suboxides. As a result, a considerable amorphization of the material surface occurred. Subsequent thermal treatment increased the crystallinity and the proportion of metallic titanium in the coating. As expected, there was a decrease in the oxygen content of the composite material, which should enhance its electrical conductivity and facilitate the application of a metal coating on the surface.

Indeed, after one hour of cathodic reduction of the nanotubes, a galvanic coating of metallic platinum uniformly forms on the material surface (Fig. 2). Thermal treatment further increases the grain size of the phases and reduces microstresses. Similarly to nanotubes or reduced nanotubes, thermal treatment leads to the formation of anatase and an increase in the proportion of metallic titanium in the composite (Table 2).

The semiconducting properties of the obtained materials are crucial as they influence the electrode potential under galvanostatic conditions. TiO_2 is classified as a wide-bandgap semiconductor. According to literature data, the band gap energies for the anatase, brookite, and rutile structures are 3.2 eV, 3.3 eV, and 3.0 eV, respectively [21].

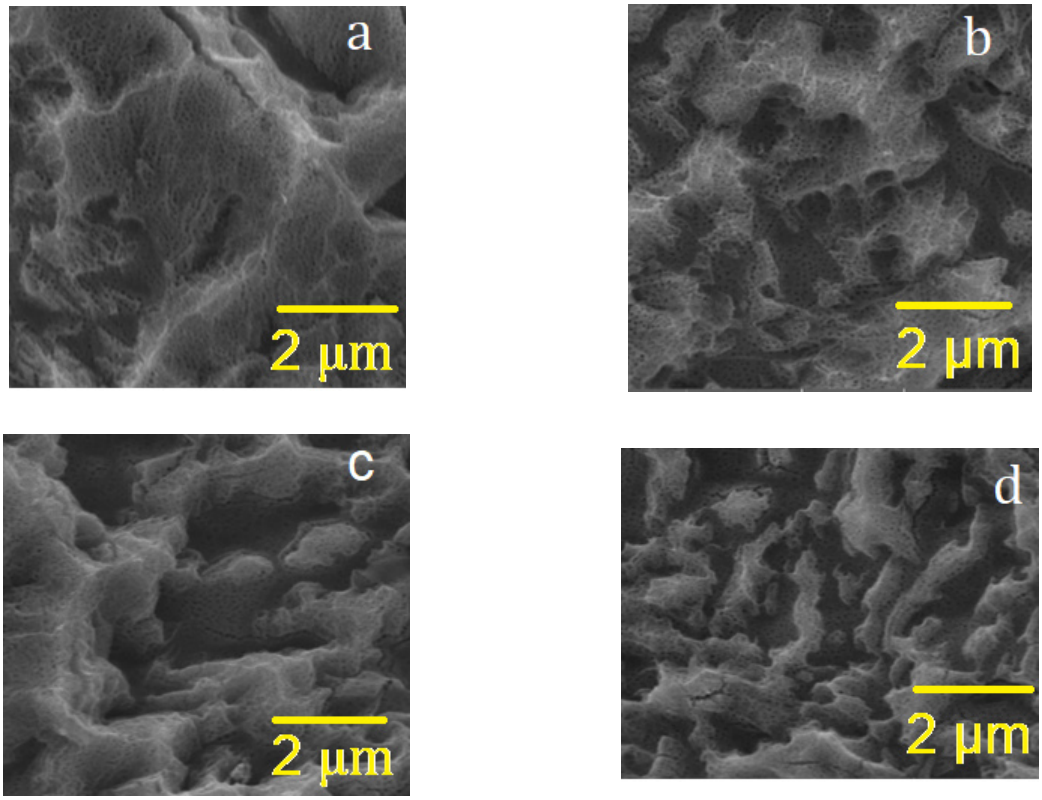

Fig. 1 SEM-images of the Ti/TiO_2 nanotubes: as prepared (a); thermally treated (b); reduced (c); reduced and thermally treated (d).

Table 1 Phase composition of the TiO_2-nanotubes.

Material	Phase composition
As prepared	TiO_2 anatase (space group $I4_1/amd$); traces of Ti (structure type Mg, space group $P6_3/mmc$)
Thermally treated	TiO_2 anatase 62.7(9) wt.%; Ti 37.3(4) wt.%
Reduced	Ti; traces of a phase with a structure of the NaCl type. Considering SEM/EDAX results it can be $TiC_{1-x}(O,F)_x$.
Reduced and thermally treated	TiO_2 anatase 57.6(9) wt.%; Ti 42.4(5) wt.%

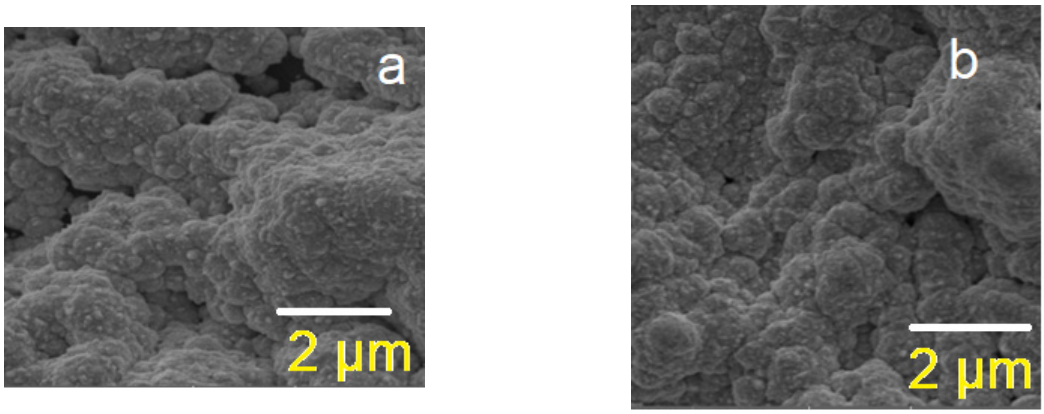

Fig. 2 SEM-images of the Ti/TiO_2-Pt nanotubes: thermally treated (a); reduced and thermally treated (b).

Table 2 Phase composition of the Pt/TiO_2-nanotubes.

Material	Phase composition
Reduced	Pt 76.9(5) wt.%; Ti 23.1(5) wt.%
Reduced and thermally treated	Pt 50.6(3) wt.%; Ti 24.4(4) wt.%; TiO_2 anatase 25.0(4) wt.%

Table 3 Semiconductor properties of the TiO_2-nanotubes.

Material	Carrier concentration $N\times10^{20}$/ cm^{-3}	Flat band potential E_{fb}/ V
As prepared	6	-0.6
Thermally treated	80	0.1
Reduced	100	0.3
Reduced and thermally treated	300	0.4
Reduced platinized	600	0.5
Reduced and thermally treated platinized	900	0.8

The electronic structure of titanium dioxide has been extensively investigated using various methods [22-24]. The valence band of TiO_2 is primarily composed of outer *p*-electrons of oxygen, while the conduction band is mainly formed by excited titanium ions [21]. The presence of partially reduced titanium (Ti^{3+}) is particularly significant for the electronic properties of titanium dioxide, with its energy level located approximately 0.2-0.8 eV below the conduction band, acting as a donor. The presence of Ti^{3+} often determines the conductivity of TiO_2.

If the near-surface region of the semiconductor electrode is depleted in charge carriers within the investigated potential range, the experimental data obtained from measuring the electrode capacitance should exhibit linearity in the $C^{-2} - E$ coordinates and follow the Mott-Schottky equation.

Preliminary studies have indicated that the materials under investigation are highly doped semiconductors ($N > 10^{18}$ cm^{-3}). Therefore, it is necessary to consider the capacitance of the Helmholtz layer C_H in the Mott-Schottky equation.

The slopes in the equations are the same, but the value of E_{fb} would consider the capacitance of the Helmholtz layer:

$$E_{fb} = E_{C^{-2}=0} + \frac{e\varepsilon\varepsilon_0 N}{2C_H^2} - \frac{kT}{e} \quad (1)$$

At an alternating current frequency of 5 Hz, the $C^{-2} - E$ dependencies for the materials under investigation exhibit linearity over a wide potential range. The carrier concentrations were determined from the slopes of the straight lines, and the flat-band potentials were obtained from the intercepts using Eq. (1). The results are presented in Table 3.

In all cases, the straight lines have positive slopes, indicating that the materials under investigation are *n*-type semiconductors. Anodic polarization of such electrodes above the potential of the flat bands will result in the depletion of carriers within the semiconductor. This, in turn, leads to a decrease in the capacitance of the semiconductor component and

an increase in the slope of the polarization curve plotted in semilogarithmic coordinates. Consequently, an increase in the potential of flat bands leads to a decrease in the overall potential, while an increase in the number of carriers results in a decrease in the slope of the polarization curve.

For comparison with materials obtained on titanium dioxide nanotubes, we examined the semiconducting properties of an oxide film produced on titanium during its thermal treatment in a tubular furnace in air at 500°C for three hours. This material is an *n*-type semiconductor with a flat-band potential of -0.6 V and a carrier concentration of 6×10^{20} cm^{-3}. The high concentration of carriers is likely attributed to the thinness of the oxide film and its non-stoichiometry, which prevents significant electron depletion at the surface due to the donor behavior of titanium metal.

During thermal treatment, the flat-band potential and carrier concentration increase, possibly due to the more crystalline structure of the material. This structural change is accompanied by an increase in the proportion of metallic titanium, which acts as an electron donor. A similar phenomenon is observed when a discontinuous platinum coating is applied to the surface of reduced nanotubes. In this case, heat treatment causes platinum migration into the bulk of the composite, which, when dispersed within the oxide, further increases the number of carriers.

Fig. 3 shows quasi-stationary current-potential curves for Ti/TiO_2-Pt electrodes in the potential range where oxygen evolution reaction (OER) takes place.

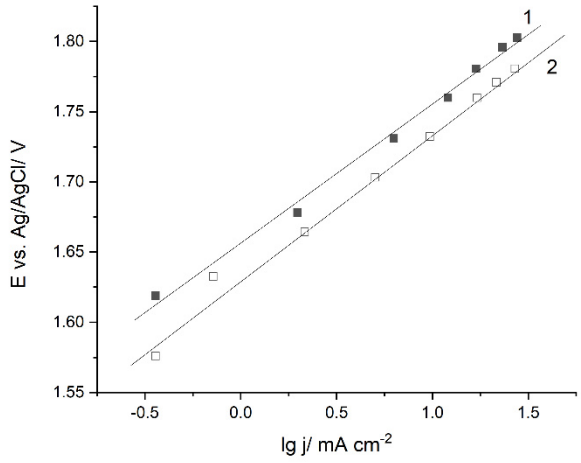

Fig. 3 Semi-logarithmic quasi steady-state polarization curves for reduced Ti/TiO_2-Pt nanotubes (1); thermally treated reduced Ti/TiO_2-Pt nanotubes (2).

The catalytic activity of the thermally treated electrode is visibly higher than that of not treated one, and much higher than that of undoped TiO_2 nanotubes. The calculated Tafel slopes were 96 and 104 mV/dec for not treated and thermally treated Ti/TiO_2-Pt samples, respectively. Such a slope may indicate the absence of a clearly defined limiting stage in the OER (electrochemical adsorption or desorption). Most likely, this phenomenon is due to the presence of two types of active site: titanium oxide and platinum. The electrocatalytic activity data of the obtained materials correlate well with their semiconducting properties.

Conclusions

A novel method was devised to deposit platinized Ti/TiO_2 nanotubes, which involves a thermal treatment stage in an air atmosphere. The results demonstrate that platinum deposition on a pre-reduced surface of nanotubes enables the production of composite coatings with enhanced electrical conductivity. Furthermore, the heat treatment of such coatings leads to a higher fraction of TiO_2 content, improved adhesion to the current collector, and increased crystallinity of the coating. Simultaneously, the internal stresses of the coating are significantly reduced.

References

[1] V.R.A. Ferreira, P.R.M. Santos, C.I.Q. Silva, M.A. Azenha, *Appl. Catal. A* 623 (2021) 118243.
[2] S. Palmas, L. Mais, M. Mascia, A. Vacca, *Curr. Opin. Electrochem.* 28 (2021) 100699.
[3] A. Kumar, N.H. Barbhuiya, S.P. Singh, *Chemosphere* 307 (2022) 135878.
[4] M. Domaschke, X. Zhou, L. Wergen, S. Romeis, M.E. Miehlich, K. Meyer, W. Peukert, P. Schmuki, *ACS Catal*. 9 (2019) 3627-3632.
[5] H. Malik, S. Sarkar, S. Mohanty, K. Carlson, *Sci. Rep.* 10 (2020) 1-11.
[6] Y. Kuroda, H. Igarashi, T. Nagai, T.W. Napporn, K. Matsuzawa, Sh. Mitsushima, K. Ota, A. Ishihara, *Electrocatalysis* 10 (2019) 459-465.
[7] B.Xu, D. Zhao, H.Y. Sohn, Y. Mohassab, B. Yang, Yu. Lan, J. Yang, *Ceram. Int.* 44 (2018) 3929-3936.
[8] E. Brillas, *Chemosphere* 286 (2022) 131849.
[9] M. Bellardita, A. Di Paola, L. Palmisano, F. Parrini, G. Buscarino, R. Amadelli, *Appl. Catal. B* 104 (2011) 291-299.
[10] X. Chen, S.S. Mao, *Chem. Rev.* 107 (2007) 2891-2959.
[11] O. Shmychkova, D. Girenko, A. Velichenko, *J. Chem. Technol. Biotechnol.* 97(4) (2022) 903-913.
[12] O. Shmychkova, T. Luk'yanenko, R. Amadelli, A. Velichenko, *J. Electroanal. Chem.* 774 (2016) 88-94.
[13] M. Chen, Sh. Pan, C. Zhang, C. Wang, W. Zhang, Z. Chen, X. Zhao, Yi. Zhao, *Chem. Eng. J.* 399 (2020) 125756.

[14] Y. Yang, M.R. Hoffmann, *Environ. Sci. Technol.* 50 (2016) 11888-11894.
[15] M. Chen, C. Wang, Y. Wang, X. Meng, Z. Chen, W. Zhang, G. Tan, *Electrochim. Acta* 323 (2019) 134779.
[16] O. Kasian, T. Luk'yanenko, A. Velichenko, R. Amadelli, *Int. J. Electrochem. Sci.* 7 (2012) 7915-7926.
[17] P.Y. Simons, F. Dachille, *Acta Crystallogr.* 23 (1967) 334-336.
[18] M. Latroche L. Brohan, R. Marchand, M. Tournoux, *J. Solid State Electrochem.* 81 (1989) 78-82.
[19] T.A. Kandiel, L. Robben, A. Alkaimad, D. Bahnemann, *Photochem. Photobiol. Sci.* 12 (2013) 602-609.
[20] M. Landmann, E. Rauls, W.G. Schmidt, *J. Condens. Matter Phys.* 24 (2012) 1-6.
[21] R. Asahi, Y. Taga, W. Mannstadt, A.J. Freeman, *Phys. Rev. B* 61 (2000) 7459-7465.
[22] V. Luca, S. Djajanti, R.F. Howe, *J. Phys. Chem. B*102 (1998) 10650-10657.
[23] R. Sanjines, H. Tang, H. Berger, F. Gozzo, G. Margaritondo, F.J. Levy, *J. Appl. Phys.* 75 (1994) 2945-2951.
[24] T.L. Thompson, J.T. Yates, *Chem. Rev.* 10 (106) 4428-4453.